

Bounds on the mass and mixing of Z' and W' bosons decaying into different pairings of W , Z , or Higgs bosons using CMS data at the LHC

P. Osland*

Department of Physics and Technology, University of Bergen, Postboks 7803, N-5020 Bergen, Norway

A. A. Pankov†

*The Abdus Salam ICTP Affiliated Centre, Technical University of Gomel, 246746 Gomel, Belarus
Institute for Nuclear Problems, Belarusian State University, 220030 Minsk, Belarus and
Joint Institute for Nuclear Research, Dubna 141980 Russia*

I. A. Serenkova‡

*The Abdus Salam ICTP Affiliated Centre, Technical University of Gomel, 246746 Gomel, Belarus
(Dated: June 6, 2022)*

The full CMS Run 2 datasets with time-integrated luminosity of 137 fb^{-1} in the diboson channels are used to probe benchmark models with extended gauge sectors such as E_6 , left-right symmetric (LR) and the sequential standard model (extended gauge model, EGM), that predict the existence of neutral Z' - and charged W' -bosons decaying to a pair of bosons WW , ZH , WZ and WH in the semileptonic final state. These benchmark models are used to interpret the results. Exclusion limits at the 95% C.L. on the Z' and W' resonance production cross section times branching ratio to electroweak gauge boson pairs in the resonance mass range between 1.0 and 4.5 TeV are here converted to constraints on Z - Z' and W - W' mixing parameters and masses. We present exclusion regions on the parameter spaces of the Z' and W' and show that the obtained exclusion regions are significantly extended compared to those derived from the previous analysis performed with Tevatron data as well as with the CMS data collected at 7 and 8 TeV in Run 1. The reported limits are the most restrictive to date.

I. INTRODUCTION

A variety of theoretical extensions to the standard model of particle physics (SM) predict new phenomena in high-energy proton-proton (pp) collisions, the discovery of which is one of the main goals of the CERN Large Hadron Collider (LHC). The LHC allows to probe new phenomena, new particles and interactions, at energies of several TeV. A wide range of models predicts the production of new heavy, TeV-scale, resonances or vector bosons decaying to pairs of SM electroweak vector bosons (jointly referred to as V in the following, with $V = W, Z$), and SM Higgs (H) bosons. Models studied in the literature include extended gauge models (EGM) [1–6], models of warped extra dimensions [7, 8], technicolour models [9, 10] associated with technirho and other technimesons, composite Higgs models [11, 12], and the heavy vector-triplet (HVT) model [13], which generalises a large number of models that predict spin-1 neutral (Z') and charged (W') resonances.

The extended gauge models are among the best motivated theoretical scenarios beyond the SM that predict the existence of new heavy neutral and charged vector bosons (Z' and W') [5, 14]. These models are considered as benchmark scenarios for diboson resonances having spin 1 ($W' \rightarrow WZ$ or WH , $Z' \rightarrow WW$ or ZH), produced predominantly via quark-antiquark annihilation ($q\bar{q}' \rightarrow W'$, $q\bar{q} \rightarrow Z'$).

The neutral and charged massive resonance production at hadron level and its subsequent decay to pairs of electroweak gauge and Higgs bosons can be expressed as

$$pp \rightarrow Z'X \rightarrow WWX, \quad (1a)$$

$$pp \rightarrow Z'X \rightarrow ZHX, \quad (1b)$$

and

$$pp \rightarrow W'X \rightarrow WZX, \quad (2a)$$

$$pp \rightarrow W'X \rightarrow WHX. \quad (2b)$$

* Per.Osland@uib.no

† pankov@ictp.it

‡ Inna.Serenkova@gmail.com

Depending on the mass and the couplings to the SM quarks and final electroweak bosons, these new states could be accessible to the LHC and observable by the ATLAS and CMS experiments [15, 16].

In the simplest models under study such as the Sequential Standard Model (SSM) [1] new neutral Z'_{SSM} and charged W'_{SSM} bosons have couplings to fermions that are identical to those of the SM Z and W bosons, but for which the trilinear couplings $Z'WW$ and $W'WZ$ are absent, $g_{Z'WW} = 0$ and $g_{W'WZ} = 0$. This suppression may arise naturally in an EGM: if the new gauge bosons and the SM ones belong to different gauge groups, a vertex such as $Z'WW$ ($W'WZ$) is forbidden. They can only be induced after symmetry breaking due to mixing of the gauge eigenstates.

Another class of models considered here are those inspired by Grand Unified Theories (GUT), which are motivated by gauge unification or a restoration of the left–right symmetry violated by the weak interaction. Examples considered in this paper include the Z' bosons of the E_6 -motivated [5] theories containing Z'_ψ , Z'_η , Z'_χ ; and high-mass neutral bosons of the left-right (LR) symmetric extensions of the SM, based on the $SU(2)_L \otimes SU(2)_R \otimes U(1)_{B-L}$ gauge group, where $B - L$ refers to the difference between baryon and lepton numbers.

The properties of possible Z' and W' bosons are also constrained by measurements of electroweak (EW) [6] processes at low energies, i.e., at energies much below their masses. Such bounds on the Z - Z' (W - W') mixing are mostly due to the constraints on deviation in Z (W) properties from the SM predictions. In particular, limits from direct hadron production with subsequent diboson decay at the Tevatron [17] and from virtual effects at LEP, through interference or mixing with the Z boson, imply that any new Z' boson is rather heavy and mixes very little with the Z boson. The measurements show that the mixing angles, referred to as $\xi_{Z-Z'}$ and $\xi_{W-W'}$, between the gauge eigenstates must be smaller than about 10^{-3} and 10^{-2} , respectively [6, 14].

Previous analyses of the Z - Z' and W - W' mixing [18–20] were carried out using the diboson production data set corresponding to the time-integrated luminosity of $\sim 36 \text{ fb}^{-1}$ collected in 2015 and 2016 with the ATLAS and CMS collaborations at $\sqrt{s} = 13 \text{ TeV}$ where, in the former case, electroweak Z and W gauge bosons decay into the semileptonic channel [21] or into the dijet final state [22]. Further updated results were obtained using the diboson and dilepton Run 2 production data set corresponding to an integrated luminosity of 139 fb^{-1} [23, 24] recorded by the ATLAS detector [25]. In the analysis presented here, we utilize the full Run 2 CMS data set on diboson resonance production published recently in Refs. [26–29] for the VV and VH channels corresponding to an integrated luminosity of 137 fb^{-1} . The present analysis includes various Z' models such as EGM (SSM), E_6 based Z_χ , Z_ψ , Z_η , as well as the Z_{LR} boson appearing in models with left-right symmetry. Also, a new set of diboson processes, $W' \rightarrow WH$ and $Z' \rightarrow ZH$, were examined.¹ Thus, our present analysis is complementary to the previous studies performed for ATLAS data in [24].

We present results as constraints on the relevant Z - Z' (W - W') mixing angle, $\xi_{Z-Z'}$ ($\xi_{W-W'}$), and on the mass $M_{Z'}$ ($M_{W'}$) and display the combined allowed parameter space for the benchmark Z' (W') boson models, showing also indirect constraints from electroweak precision data (EW), previous direct search constraints from the Tevatron and from the LHC with 7 and 8 TeV in Run 1 (where available), as well as those obtained from the LHC at 13 TeV with the full CMS Run 2 data set of time-integrated luminosity of 137 fb^{-1} in the semileptonic [26–29] final states.

The paper is organized as follows. In Sect. II we present the theoretical framework, then, in Sects. III and IV we review the production and decay of W' and Z' , respectively. Finally, Sect. V contains concluding remarks. The paper is a follow-up study of our earlier analysis of the corresponding ATLAS data [24]. In order to make it self-contained, there is some repetition of basic formulas.

II. V - V' MIXING

As mentioned above, in the SSM, the coupling constants of the W' and Z' bosons with SM fermions are identical to the corresponding SM couplings, while the W' and Z' couplings to, respectively, WZ and WW vanish, $g_{W'WZ} = g_{Z'WW} = 0$. Such a suppression may arise in an EGM in a natural manner: if the new gauge bosons and those of the SM belong to different gauge groups, vertices such as $W'WZ$ and $Z'WW$ do not arise. They can only occur after symmetry breaking due to mixing of the gauge eigenstates. Triple gauge boson couplings (such as $W'WZ$ and $Z'WW$) as well as the vector-vector-scalar couplings (like $W'WH$ and $Z'ZH$) arise from the symmetry breaking and may contribute to the W' and Z' decays, respectively. The vertices are then suppressed by a factor of the order of $(M_W/M_{V'})^2$, where V' represents a W' or a Z' boson.

In an EGM [1], the trilinear gauge boson couplings are modified by mixing factors

$$\xi_{V-V'} = \mathcal{C} \times (M_W/M_{V'})^2, \quad (3)$$

¹ We do not consider here effects of bosonic mixing in dilepton production [24] as it is out of scope of the present paper.

where \mathcal{C} is a scaling constant that sets the coupling strength. Note that the EGM can be parametrized either in terms of $(M_{V'}, \mathcal{C})$ or in terms of $(M_{V'}, \xi_{V-V'})$. Specifically, in an EGM the standard-model trilinear gauge boson coupling strength g_{WWZ} ($= e \cot \theta_W$), is replaced by $g_{W'WZ} = \xi_{W-W'} \cdot g_{WWZ}$ in the WZ channel and $g_{Z'WW} = \xi_{Z-Z'} \cdot g_{WWZ}$ in the WW channel. Following the parametrization of the trilinear gauge boson couplings $W'WZ$ and $Z'WW$ presented in [17] for the analysis and interpretation of the CDF data on $p\bar{p} \rightarrow W'X \rightarrow WZX$ and $p\bar{p} \rightarrow Z'X \rightarrow W^+W^-X$, expressed in terms of two free parameters,² $\xi_{W-W'}$ ($\xi_{Z-Z'}$) and $M_{W'}$ ($M_{Z'}$), we will set two-dimensional limits, by using the CMS resonant diboson production data [26–29] collected in the full Run 2 data set with time-integrated luminosity of 137 fb^{-1} . The presented analysis in the EGM with two free parameters is more general than the previous ones where the only parameter is the V' mass. As for the SSM, one has $V'_{\text{SSM}} \equiv V'_{\text{EGM}}$ when $\xi_{V-V'} = 0$.

Note that the parametrization of boson mixing introduced by Altarelli et al. [1], though being simplified, has a well-motivated theoretical basis. To be specific, we briefly consider Z^0 - $Z^{0'}$ mixing within the framework of models with extended gauge sector (see, e.g. [3–6]). The mass eigenstates Z and Z' are admixtures of the weak eigenstates Z^0 of $SU(2) \times U(1)$ and $Z^{0'}$ of the extra $U(1)'$, respectively:

$$Z = Z^0 \cos \phi + Z^{0'} \sin \phi, \quad (4a)$$

$$Z' = -Z^0 \sin \phi + Z^{0'} \cos \phi. \quad (4b)$$

In each case there is a relation between the Z^0 - $Z^{0'}$ mixing angle ϕ and the masses M_Z and $M_{Z'}$ [5]:

$$\tan^2 \phi = \frac{M_{Z^0}^2 - M_Z^2}{M_{Z'}^2 - M_{Z^0}^2} \simeq \frac{2 M_{Z^0} \Delta M_{Z^0 Z}}{M_{Z'}^2}, \quad (5)$$

where the downward shift $\Delta M_{Z^0 Z} = M_{Z^0} - M_Z > 0$, and M_{Z^0} is the mass of the Z boson in the absence of mixing, i.e., for $\phi = 0$, given by

$$M_{Z^0} = \frac{M_W}{\sqrt{\rho_0} \cos \theta_W}, \quad (6)$$

in terms of the charged (M_W) gauge boson mass and the ρ_0 parameter. The mixing angle ϕ will play an important role in our analysis. Such mixing effects reflect the underlying gauge symmetry and/or the structure of the Higgs sector of the model as the ρ_0 parameter depends on the ratios of the Higgs vacuum expectation values and on the total and third components of weak isospin of the Higgs fields. For each type of $Z^{0'}$ boson, defined by its gauge couplings, there are three classes of models, which differ in the assumptions concerning the quantum numbers of the Higgs fields which generate the Z -boson mass matrix [3–5]:

- (i) The least constrained (ρ_0 free) model makes no assumption concerning the Higgs sector. It allows arbitrary $SU(2)$ representations for the Higgs fields, and is the analogue of allowing $\rho_0 \neq 1$ in the $SU(2) \times U(1)$ model. In this case M_Z , $M_{Z'}$ and ϕ are all free parameters.
- (ii) If one assumes that all $SU(2)$ breaking is due to Higgs doublets and singlets ($\rho_0 = 1$ model), there are only two free parameters, which we identify as ϕ and $M_{Z'}$. We will adopt this parametrization throughout the paper.
- (iii) Finally, in specific models one specifies not only the $SU(2)$ assignments but the $U(1)'$ assignments of the Higgs fields. Since the same Higgs multiplets generate both M_Z and ϕ , one has an additional constraint. To a good approximation, for $M_Z \ll M_{Z'}$, in specific “minimal-Higgs models”, one has an additional constraint [30, 31]

$$\phi \simeq -s_W^2 \frac{\sum_i \langle \Phi_i \rangle^2 I_{3L}^i Q'_i}{\sum_i \langle \Phi_i \rangle^2 (I_{3L}^i)^2} = P \frac{M_Z^2}{M_{Z'}^2}, \quad (7)$$

where s_W is the sine of the electroweak angle. In these models ϕ and $M_{Z'}$ are not independent and there is only one (e.g., $M_{Z'}$) free parameter. This parametrization is of the form presented in Eq. (3). Furthermore, $\langle \Phi_i \rangle$ are the Higgs (doublet) vacuum expectation values spontaneously breaking the symmetry, and Q'_i are their charges with respect to the additional $U(1)'$. In these models the same Higgs multiplets are responsible for both generation of the mass M_Z and for the strength of the Z^0 - $Z^{0'}$ mixing. Thus P is a model-dependent constant.

² Such W' and Z' , described in terms of two parameters (mass and mixing), are here referred to as EGM bosons.

This Z^0 - $Z^{0'}$ mixing induces a change in the couplings of the two bosons to fermions. From Eq. (4), one obtains the vector and axial-vector couplings of the Z and Z' bosons to fermions:

$$v_f = v_f^0 \cos \phi + v_f^{0'} \sin \phi, \quad a_f = a_f^0 \cos \phi + a_f^{0'} \sin \phi, \quad (8a)$$

$$v_f' = v_f^{0'} \cos \phi - v_f^0 \sin \phi, \quad a_f' = a_f^{0'} \cos \phi - a_f^0 \sin \phi, \quad (8b)$$

with unprimed and primed couplings referring to Z^0 and $Z^{0'}$, respectively, and found, e.g. in [3–5].

An important property of the models under consideration is that the gauge eigenstate $Z^{0'}$ does not couple to the W^+W^- pair since it is neutral under $SU(2)$. Therefore the W -pair production is sensitive to a Z' only to the extent that there is a non-zero Z^0 - $Z^{0'}$ mixing. From Eq. (4), one obtains:

$$g_{WWZ} = \cos \phi g_{WWZ^0}, \quad (9a)$$

$$g_{WWZ'} = -\sin \phi g_{WWZ^0}, \quad (9b)$$

where $g_{WWZ^0} = e \cot \theta_W$. Also, $g_{WW\gamma} = e$.

In many extended gauge models, while the couplings to fermions are not much different from those of the SM, the $Z'WW$ coupling is substantially suppressed with respect to that of the SM. In fact, in the extended gauge models the SM trilinear gauge boson coupling strength, g_{WWZ^0} , is replaced by $g_{WWZ^0} \rightarrow \xi_{Z-Z'} \cdot g_{WWZ^0}$, where $\xi_{Z-Z'} \equiv |\sin \phi|$ (see Eq. (9b)) is the mixing factor. We will set cross section limits on such Z' as functions of the mass $M_{Z'}$ and $\xi_{Z-Z'}$.

In addition, we study W - W' mixing in the processes (2a) and (2b) within the framework of the EGM model [1, 2]. Mass mixing may be induced between the electrically charged gauge bosons at the tree level. The physical (mass) eigenstates of W and W' are admixtures of the weak eigenstates denoted as \hat{W} and \hat{W}' , respectively, and obtained by a rotation of those fields [14, 32, 33]:

$$W^\pm = \hat{W}^\pm \cos \theta_{WW'} + \hat{W}'^\pm \sin \theta_{WW'}, \quad (10a)$$

$$W'^\pm = -\hat{W}^\pm \sin \theta_{WW'} + \hat{W}'^\pm \cos \theta_{WW'}, \quad (10b)$$

in analogy with Eq. (4). Upon diagonalization of their mass matrix, the couplings of the observed W boson are shifted from the SM values. The mixing parameter $\xi_{W-W'}$ between gauge eigenstates can be defined as $\xi_{W-W'} \equiv |\sin \theta_{WW'}|$.

III. HADRON PRODUCTION AND DECAY OF W' BOSON

In this section, we consider the simplest EGM model which predicts charged heavy gauge bosons. At the lowest order in the EGM, W' production and decay into WZ and WH in proton-proton collisions occur through quark-antiquark annihilation in the s -channel. Adopting the Narrow-Width Approximation (NWA), one can factorize the processes (2a) and (2b) into the W' production and the W' decay,

$$\sigma(pp \rightarrow W'X \rightarrow WZX) = \sigma(pp \rightarrow W'X) \times \text{BR}(W' \rightarrow WZ), \quad (11a)$$

$$\sigma(pp \rightarrow W'X \rightarrow WHX) = \sigma(pp \rightarrow W'X) \times \text{BR}(W' \rightarrow WH). \quad (11b)$$

Here, $\sigma(pp \rightarrow W'X)$ is the total (theoretical) W' production cross section, $\text{BR}(W' \rightarrow WZ) = \Gamma_{W'}^{WZ}/\Gamma_{W'}$ and similarly $\text{BR}(W' \rightarrow WH) = \Gamma_{W'}^{WH}/\Gamma_{W'}$ with $\Gamma_{W'}$ the total width of the W' .

A. The W' width

In the EGM the W' bosons can decay into pairs of SM fermions (charged leptons, neutrinos and quarks), gauge bosons WZ and WH . Specifically, in the calculation of the total width $\Gamma_{W'}$ we consider the following channels: $W' \rightarrow f\bar{f}'$, WZ , and WH , where f is a SM fermion ($f = \ell, \nu, q$). Note, that here the ℓ includes τ leptons as well. Only the familiar left-handed neutrinos are considered, possible right-handed exotic neutrinos are assumed to be kinematically unavailable as final states. Also, we shall ignore the couplings to other beyond-SM particles such as SUSY partners and exotic fermions. As a result, the total decay width of the W' boson is taken to be

$$\Gamma_{W'} = \sum_f \Gamma_{W'}^{f\bar{f}'} + \Gamma_{W'}^{WZ} + \Gamma_{W'}^{WH}. \quad (12)$$

The presence of the last two decay channels, which are often neglected at low and moderate values of $M_{W'}$, is due to W - W' mixing which is constrained to be tiny. In particular, for the range of $M_{W'}$ values below ~ 2 TeV, the dependence of $\Gamma_{W'}$ on the values of $\xi_{W-W'}$ (within its allowed range) induced by $\Gamma_{W'}^{WZ}$ and $\Gamma_{W'}^{WH}$ is unimportant because $\sum_f \Gamma_{W'}^{f\bar{f}'}$ highly dominates over the diboson partial widths as illustrated in Fig. 1 for a representative value of the mixing parameter. Therefore, in this mass range, one can approximate the total width as $\Gamma_{W'} \approx \sum_f \Gamma_{W'}^{f\bar{f}'} = 3.5\% \times M_{W'}$ [20], where the sum runs over SM fermions only. For heavier W' bosons, the diboson decay channels, WZ and WH , start to play an important role, and we are no longer able to ignore them [20, 23]. To be specific, we assume that both partial widths are comparable, $\Gamma_{W'}^{WH} \simeq \Gamma_{W'}^{WZ}$ for heavy $M_{W'}$, as required by the Equivalence theorem [34].

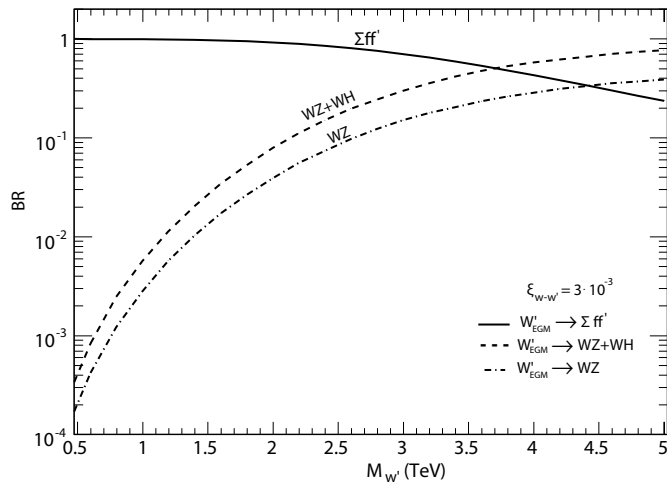


FIG. 1. Branching ratios $\text{BR}(W' \rightarrow \sum f\bar{f}')$ (solid), $\text{BR}(W' \rightarrow WZ)$ (dash-dotted), and $\text{BR}(W' \rightarrow WZ + WH)$ (dashed) vs $M_{W'}$ in the EGM where the W - W' mixing factor is taken to be $\xi_{W-W'} = 3 \cdot 10^{-3}$. It is assumed that $\text{BR}(W' \rightarrow WZ) = \text{BR}(W' \rightarrow WH)$.

The partial width of the $W' \rightarrow WZ$ decay channel in the EGM can be written as [1, 20, 24]:

$$\Gamma_{W'}^{WZ} = \frac{\alpha_{\text{em}}}{48} \cot^2 \theta_W M_{W'} \frac{M_{W'}^4}{M_W^2 M_Z^2} \left[\left(1 - \frac{M_Z^2 - M_W^2}{M_{W'}^2} \right)^2 - 4 \frac{M_W^2}{M_{W'}^2} \right]^{3/2} \times \left[1 + 10 \left(\frac{M_W^2 + M_Z^2}{M_{W'}^2} \right) + \frac{M_W^4 + M_Z^4 + 10 M_W^2 M_Z^2}{M_{W'}^4} \right] \cdot \xi_{W-W'}^2. \quad (13)$$

For a fixed mixing factor $\xi_{W-W'}$ and at large $M_{W'}$, the total width increases rapidly with the W' mass because of the quintic dependence of the WZ mode on the W' mass $\Gamma_{W'}^{WZ} \propto M_{W'} [M_{W'}^4 / (M_W^2 M_Z^2)]$, corresponding to the production of longitudinally polarized W and Z in the channel $W' \rightarrow W_L Z_L$ [1]. In this case, the WZ mode (as well as WH) becomes dominant and $\text{BR}(W' \rightarrow WZ) \rightarrow 0.5$, while the fermionic decay channels, $\sum_f \Gamma_{W'}^{f\bar{f}'} \propto M_{W'}$, are increasingly suppressed, as illustrated in Fig. 1.

B. Constraints on W - W' mixing and $M_{W'}$

The data we consider were collected with the CMS detector during the 2015–2018 running period of the LHC, referred to as Run 2 and correspond to a time-integrated luminosity of 137 fb^{-1} . The CMS experiment has presented the recent search for diboson resonances based on the full Run 2 data set in the semileptonic final states [26–29] and set limits on the W' production cross sections times branching fraction in the processes $pp \rightarrow W'X \rightarrow WZX$ and $pp \rightarrow W'X \rightarrow WHX$ for $M_{W'}$ in the 1.0 TeV – 4.5 TeV range.

Such a search has also been presented by the ATLAS Collaboration using 139 fb^{-1} of data recorded for the $W' \rightarrow WZ$ channel at $\sqrt{s} = 13 \text{ TeV}$ [25], and exclusion limits at the 95% C.L. on the W' resonance production cross section times branching ratio to electroweak gauge boson pairs WZ in the resonance mass range between $\simeq 0.5 \text{ TeV}$ and 5 TeV. These data were similarly converted to constraints on the W - W' mixing parameter and $M_{W'}$ mass [24].

In Fig. 2, we show the observed 95% C.L. upper limits on the production cross section times the branching fraction, $\sigma_{95\%} \times \text{BR}(W' \rightarrow WZ)$ (left panel) and $\sigma_{95\%} \times \text{BR}(W' \rightarrow WH)$ (right panel), as functions of the W' mass.

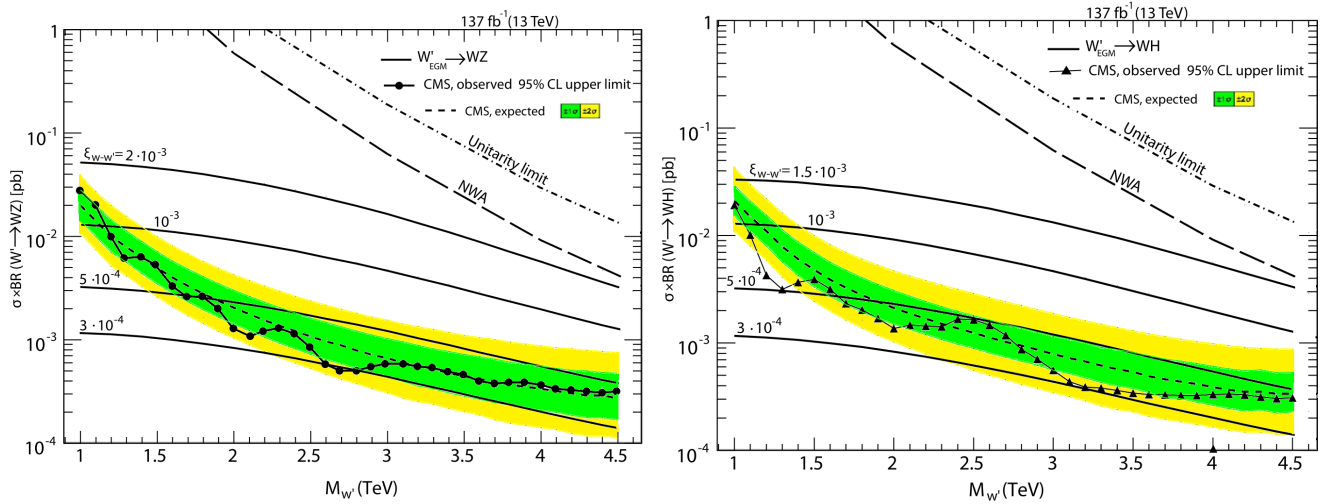


FIG. 2. Left panel: Observed and expected 95% C.L. upper limits on $\sigma_{95\%} \times \text{BR}(W' \rightarrow WZ)$, showing CMS data on the semileptonic final states for 137 fb^{-1} [26, 27]. The inner (green) and outer (yellow) bands around the expected limits representing $\pm 1\sigma$ and $\pm 2\sigma$ uncertainties, respectively, as determined by CMS. The theoretical production cross sections $\sigma(pp \rightarrow W'X) \times \text{BR}(W' \rightarrow WZ)$ for the EGM are shown by solid curves with mixing factors $\xi_{W-W'}$ attached to the curves [24]. The NWA and unitarity constraints are also shown [20, 35]. Right panel: Same as in the left panel but for the process $pp \rightarrow W' \rightarrow WH$ [28, 29].

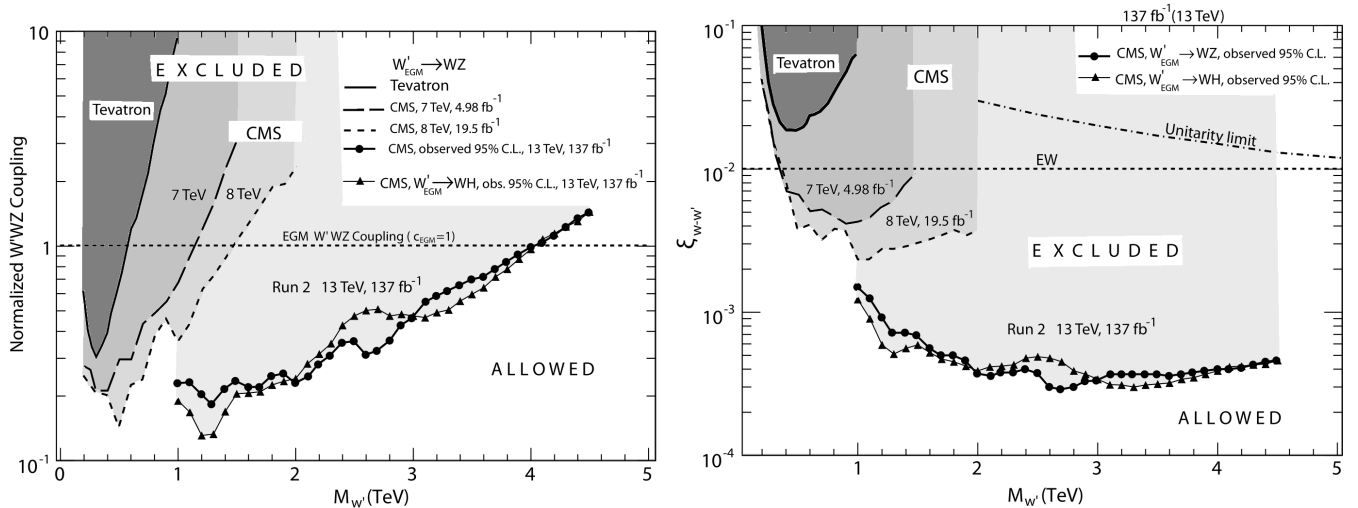


FIG. 3. Left panel: Upper limit at 95% C.L. on the strength of the $g_{W'WZ}$ coupling normalized to the EGM trilinear gauge coupling of $g_{W'WZ}$ for $\mathcal{C} = 1$, as a function of the W' mass, obtained from direct search constraints from the Tevatron in $p\bar{p} \rightarrow WZX$ (dark shaded area) as well as from the LHC searches for $pp \rightarrow WZX$ at 7 TeV and 8 TeV (Run 1) (respectively, dark and light gray areas) and at 13 TeV from diboson production of $W' \rightarrow WZ$ and $W' \rightarrow WH$ in semileptonic final state using the full Run 2 CMS data set. The regions above each curve for the WZ and WH channels are excluded. Right panel: Same as in the left panel but in the $(M_{W'}, \xi_{W-W'})$ plane.

The theoretical production cross sections multiplied by the branching ratio of W' into WZ/WH bosons, $\sigma(pp \rightarrow W'X) \times \text{BR}(W' \rightarrow WZ/WH)$, as functions of the two parameters $(M_{W'}, \xi_{W-W'})$ can be found in [20, 24] and are here compared with the limits established by the CMS experiment, $\sigma_{95\%} \times \text{BR}(W' \rightarrow WZ/WH)$ [26, 27]. The simulation of signals for the EGM W' is based on an adapted version of the leading-order PYTHIA 8.2 event generator [36]. A

mass-dependent K factor is adopted to rescale the LO PYTHIA prediction to the the NNLO one, using the ZWPROD [37] software. The factorization and renormalization scales are both set to the W' mass.

The area below the long-dashed curve labelled “NWA” corresponds to the region where the W' resonance width is predicted to be less than 5% of its mass, corresponding to the best detector resolution of the searches, where the narrow-width assumption is satisfied. We also show a curve labelled “Unitarity limit” that corresponds to the unitarity bound (see, e.g. [20, 24, 35]).

The theoretical curves for the cross sections $\sigma(pp \rightarrow W'X) \times \text{BR}(W' \rightarrow WZ)$, in descending order, correspond to values of the W - W' mixing factor $\xi_{W-W'}$ from 0.002 to 0.0003. Similarly, $\sigma(pp \rightarrow W'X) \times \text{BR}(W' \rightarrow WH)$ is shown with $\xi_{W-W'}$ from 0.0015 to 0.0003. The intersection points of the measured upper limits on the production cross section with these theoretical cross sections for various values of $\xi_{W-W'}$ give the corresponding upper bounds on $\xi_{W-W'}$, displayed in Fig. 3.

From the comparison of sensitivities of the processes (2a) and (2b) to W' with different decay channels illustrated in Fig. 3, one can conclude that the sensitivity of the $W' \rightarrow WZ$ channel is quite comparable with that for the $W' \rightarrow WH$ channel within the whole range of the W' mass, from 1.0 TeV to 4.5 TeV. These features are illustrated in Fig. 3. Notice that the two panels of Fig. 3 provide the same information. The different types of plots presented in those panels based on the specific parametrization of the W - W' mixing employed there, namely expressed in terms of a normalized $g_{W'WZ}$ coupling [38–40] (left panel) and, alternatively in terms of the mixing parameter $\xi_{W-W'}$ (right panel). Throughout the paper we use the latter one proposed by CDF [17] and exploited in previous analyses of ATLAS data sets [20, 23, 24].

For reference, we display limits on the W' parameters from the Tevatron (CDF) [17] as well as from CMS obtained at 7 and 8 TeV of LHC data taking in Run 1 [20, 24]. Fig. 3 (right panel) shows that the CDF experiment at the Tevatron [17] excludes EGM W' bosons with $\xi_{W-W'} \gtrsim 2 \cdot 10^{-2}$ in the resonance mass range $0.25 \text{ TeV} < M_{W'} < 1 \text{ TeV}$ at the 95% C.L., whereas CMS at LHC in Run 1 improved those constraints, excluding W' boson parameters at $\xi_{W-W'} \gtrsim 2 \cdot 10^{-3}$ in the mass range $0.2 \text{ TeV} < M_{W'} < 2 \text{ TeV}$.

As expected, the increase of the time-integrated luminosity up to 137 fb^{-1} leads to increased sensitivity of the diboson channels under study over the whole mass range of $1.0 \text{ TeV} < M_{W'} < 4.5 \text{ TeV}$ and allows to set stronger constraints on the mixing angle $\xi_{W-W'}$, excluding $\xi_{W-W'} > 2.5 \cdot 10^{-4}$ as shown in Fig. 3 (right panel). Our results extend the sensitivity much beyond the corresponding CDF Tevatron results [17] as well as the ATLAS and CMS sensitivity attained at 7 and 8 TeV. Also, for the first time, we set W' limits as functions of the mass $M_{W'}$ and mixing factor $\xi_{W-W'}$ from the study of the diboson production and subsequent decay into semileptonic final states at the LHC at 13 TeV with the full CMS Run 2 data set. The exclusion region obtained in this way on the parameter space of the W' naturally supersedes the corresponding exclusion area obtained for time-integrated luminosity of 36.1 fb^{-1} at CMS in the semileptonic channel as reported in [18]. The limits on the W' parameters presented in this section obtained from the diboson WZ and WH production in semileptonic final states, corresponding to a time-integrated luminosity of 137 fb^{-1} , are quite complementary to those obtained with the entire ATLAS Run 2 data set [24] and the best to date.

IV. HADRON PRODUCTION AND DECAY OF Z' BOSON

We shall next consider Z' boson production in pp collision and its subsequent decay into diboson channels, $Z' \rightarrow W^+W^-$ and $Z' \rightarrow ZH$. Specifically, we concentrate on the models with extended gauge sector predicting the existence of Z' bosons, such as E_6 , left-right symmetric LR and the EGM. The processes under study are:

$$\sigma(pp \rightarrow Z'X \rightarrow W^+W^-X) = \sigma(pp \rightarrow Z'X) \times \text{BR}(Z' \rightarrow W^+W^-), \quad (14a)$$

$$\sigma(pp \rightarrow Z'X \rightarrow ZHX) = \sigma(pp \rightarrow Z'X) \times \text{BR}(Z' \rightarrow ZH). \quad (14b)$$

Here, $\sigma(pp \rightarrow Z'X)$ is the total (theoretical) Z' production cross section, $\text{BR}(Z' \rightarrow W^+W^-) = \Gamma_{Z'}^{WW}/\Gamma_{Z'}$ and $\text{BR}(Z' \rightarrow ZH) = \Gamma_{Z'}^{ZH}/\Gamma_{Z'}$ with $\Gamma_{Z'}$ the total width of the Z' . Among the Z' models, we start out with a discussion of the EGM.

A. The Z' width

In the computation of the total width $\Gamma_{Z'}$ we take into account the following channels: $Z' \rightarrow f\bar{f}$, W^+W^- , and ZH [15, 16, 23, 24], where H is the SM Higgs boson and f refers to the SM fermions ($f = l, \nu, q$). Throughout the paper we shall ignore the couplings of the Z' to any beyond-SM particles such as right-handed neutrinos, as well as to SUSY partners and any other exotic fermions. Any additional states may increase the width of the Z' .

The total width $\Gamma_{Z'}$ of the Z' boson can then be written as follows:

$$\Gamma_{Z'} = \sum_f \Gamma_{Z'}^{ff} + \Gamma_{Z'}^{WW} + \Gamma_{Z'}^{ZH}. \quad (15)$$

The two last terms are due to Z - Z' mixing. For the range of $M_{Z'}$ values below ~ 3 TeV, the dependence of $\Gamma_{Z'}$ on the values of $\xi_{Z-Z'}$ (within its allowed range) is unimportant. Therefore, in this mass range, one can approximate the total width as $\Gamma_{Z'} \approx \sum_f \Gamma_{Z'}^{ff}$, where the sum runs over SM fermions only. Within the approximation above, one can quantify the ratio of $\Gamma_{Z'}/M_{Z'}$ for the benchmark EGM as 3%, whereas for the ψ , η , χ and LR models it varies from 0.5% to 2.0%.

However, for larger Z' masses, $M_{Z'} > 4$ TeV, there is an enhancement in the coupling that cancels the suppression due to the tiny Z - Z' mixing parameter $\xi_{Z-Z'}$ [15]. We note that the ‘‘Equivalence theorem’’ [34] suggests a value for $\text{BR}(Z' \rightarrow ZH)$ comparable to $\text{BR}(Z' \rightarrow W^+W^-)$, up to electroweak symmetry breaking effects and phase-space factors. Throughout this paper, for definiteness, we adopt a scenario where both partial widths are comparable, $\Gamma_{Z'}^{ZH} \simeq \Gamma_{Z'}^{WW}$ for heavy $M_{Z'}$ [41–43].

For all $M_{Z'}$ values of interest for our analysis the width of the Z' boson is considerably smaller than the experimental mass resolution ΔM . We adopt the approximation $\Delta M/M \approx 5\%$, as reported, e.g., in [44] for reconstructing the diboson invariant mass of the W^+W^- and ZH systems.

The partial width of the $Z' \rightarrow W^+W^-$ decay channel can be written as [1]:

$$\Gamma_{Z'}^{WW} = \frac{\alpha_{\text{em}}}{48} \cot^2 \theta_W M_{Z'} \left(\frac{M_{Z'}}{M_W} \right)^4 \left(1 - 4 \frac{M_W^2}{M_{Z'}^2} \right)^{3/2} \left[1 + 20 \left(\frac{M_W}{M_{Z'}} \right)^2 + 12 \left(\frac{M_W}{M_{Z'}} \right)^4 \right] \cdot \xi_{Z-Z'}^2. \quad (16)$$

For a fixed mixing factor $\xi_{Z-Z'}$ and at large $M_{Z'}$ where $\Gamma_{Z'}^{WW}$ dominates over $\sum_f \Gamma_{Z'}^{ff}$, the total width increases rapidly with the mass $M_{Z'}$ because of the quintic dependence of the W^+W^- mode on the Z' mass. In this case, the W^+W^- mode (together with $Z' \rightarrow ZH$) becomes dominant and $\text{BR}(Z' \rightarrow W^+W^-) \rightarrow 0.5$ (this value arises from the assumption $\Gamma_{Z'}^{ZH} = \Gamma_{Z'}^{WW}$), while the fermionic decay channels ($\Gamma_{Z'}^{ff} \propto M_{Z'}$) are increasingly suppressed. These features are illustrated in Fig. 4, where we plot $\text{BR}(Z' \rightarrow W^+W^-)$, $\text{BR}(Z' \rightarrow W^+W^- + ZH)$ and $\text{BR}(Z' \rightarrow \sum_f \bar{f}f)$ vs $M_{Z'}$ for the Z'_{EGM} taking $\xi_{Z-Z'} = 3 \cdot 10^{-3}$ as a representative case.

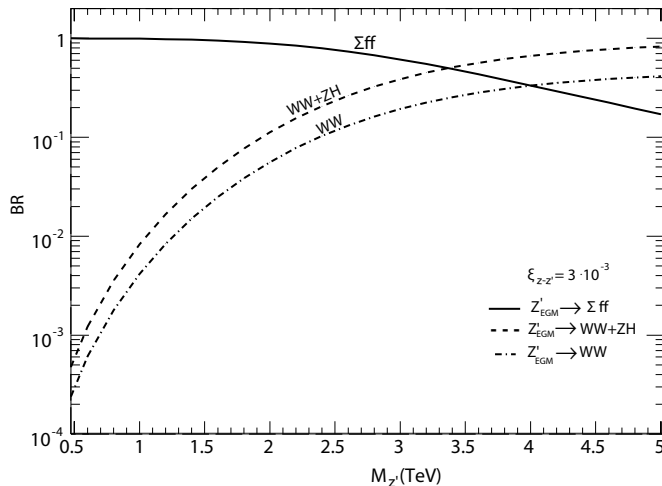


FIG. 4. Branching ratios $\text{BR}(Z' \rightarrow \sum_f \bar{f}f)$ (solid), $\text{BR}(Z' \rightarrow W^+W^-)$ (dash-dotted), and $\text{BR}(Z' \rightarrow W^+W^- + ZH)$ (dashed) vs $M_{Z'}$ in the EGM for a Z - Z' mixing factor $\xi_{Z-Z'} = 3 \cdot 10^{-3}$. It is assumed that $\text{BR}(Z' \rightarrow W^+W^-) = \text{BR}(Z' \rightarrow ZH)$.

B. Constraints on Z - Z' mixing and $M_{Z'}$

In Fig. 5, we consider the full CMS Run2 data set of time integrated luminosity of 137 fb^{-1} and show the observed 95% C.L. upper limits on the production cross section times the branching fraction, $\sigma_{95\%} \times \text{BR}(Z' \rightarrow W^+W^-)$ (left

panel) and $\sigma_{95\%} \times \text{BR}(Z' \rightarrow ZH)$ (right panel), as functions of the Z' mass, obtained from the semileptonic [26–29] final state. These figures allow to make a comparison of the sensitivities of the data to the Z - Z' mixing parameter and new gauge boson mass and they demonstrate the comparable sensitivity to Z' of the W^+W^- and ZH channels over almost the whole allowed Z' mass range. However, as can be seen from Fig. 5, the Z' mass range in the ZH channel is somewhat broader than that of the W^+W^- channel, namely 0.8–5.0 TeV vs 1.0–4.5 TeV, respectively.

Then, for Z'_{EGM} we compute the theoretical LHC production cross section multiplied by the branching ratios into two W^\pm bosons and into ZH , $\sigma(pp \rightarrow Z'_{\text{EGM}}X) \times \text{BR}(Z'_{\text{EGM}} \rightarrow W^+W^-)$ [23, 24] and $\sigma(pp \rightarrow Z'_{\text{EGM}}X) \times \text{BR}(Z'_{\text{EGM}} \rightarrow ZH)$, as functions of the two parameters $(M_{Z'}, \xi_{Z-Z'})$, and compare them with the limits established by the CMS experiments, $\sigma_{95\%} \times \text{BR}(Z' \rightarrow W^+W^-)$ (left panel) [26, 27] and $\sigma_{95\%} \times \text{BR}(Z' \rightarrow ZH)$ (right panel) [28, 29].

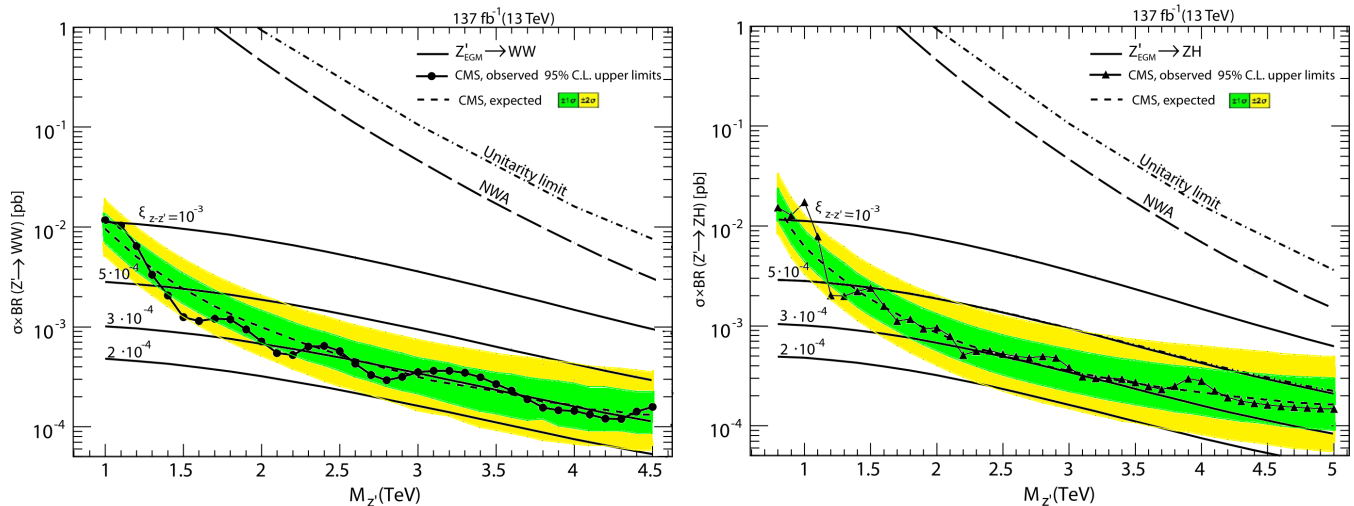


FIG. 5. Left panel: 95% C.L. upper limits on $\sigma_{95\%} \times \text{BR}(Z' \rightarrow WW)$, showing CMS data on the semileptonic final states for 137 fb^{-1} [26, 27]. The theoretical production cross sections $\sigma(pp \rightarrow Z'X) \times \text{BR}(Z' \rightarrow WW)$ for the EGM are calculated from PYTHIA with a Z' mass-dependent K -factor, given by solid curves, for mixing factor $\xi_{Z-Z'}$ ranging from 10^{-3} and down to $2 \cdot 10^{-4}$. The NWA and unitarity constraints are also shown. Right panel: Same as in the left panel but for the process $pp \rightarrow Z' \rightarrow ZH$ [28, 29].

The theoretical production cross sections $\sigma(pp \rightarrow Z'_{\text{EGM}}) \times \text{BR}(Z'_{\text{EGM}} \rightarrow W^+W^-)$ for Z'_{EGM} boson are calculated from a dedicated modification of PYTHIA 8.2 [36]. Higher-order QCD corrections to the signal were estimated using a K -factor, for which we adopt a mass-independent value of 1.9 [45–47]. These theoretical curves for the cross sections, in descending order, correspond to values of the Z - Z' mixing factor $\xi_{Z-Z'}$ ranging from 10^{-3} and down to $2 \cdot 10^{-4}$. The NWA and unitarity constraints are also shown [23, 24, 35]. The intersection points of the measured upper limits on the production cross section with this theoretical cross section for various values of $\xi_{Z-Z'}$ give the corresponding bounds on $(M_{Z'}, \xi_{Z-Z'})$, presented in Fig. 6.

Different bounds on the Z' parameter space are collected in Fig. 6 for the Z'_{EGM} model, showing that at high masses, the limits on $\xi_{Z-Z'}$ obtained from the full Run 2 data set collected at $\sqrt{s} = 13 \text{ TeV}$ and recorded by the CMS detector are substantially stronger than that derived from the global analysis of the precision electroweak data (EW) [6], as well as the limits obtained from diboson data at the Tevatron [17]. Limits obtained separately with CMS from the two channels, $Z' \rightarrow W^+W^-$ and $Z' \rightarrow ZH$, are shown for comparison. It turns out that the diboson channel $Z' \rightarrow ZH$, in contrast to $Z' \rightarrow W^+W^-$, allows to place limits on Z - Z' mixing in the narrow mass ranges such as $0.8 \text{ TeV} \leq M_{Z'} \leq 1.0 \text{ TeV}$ and $4.5 \text{ TeV} \leq M_{Z'} \leq 5.0 \text{ TeV}$, whereas in the rest of the resonance mass range, $1.0 \text{ TeV} \leq M_{Z'} \leq 4.5 \text{ TeV}$, both channels demonstrate comparable sensitivity to Z - Z' mixing.

The analysis of Z - Z' mixing, performed here for the EGM, can also be carried out for the other benchmark models. The results of the numerical analysis for these models are shown in Figs. 7–10. Limits on a Z'_{model} are calculated as the intersection between the observed limits, $\sigma_{95\%} \times \text{BR}(Z' \rightarrow W^+W^-)$ and $\sigma_{95\%} \times \text{BR}(Z' \rightarrow ZH)$, with the model prediction, $\sigma(pp \rightarrow Z'_{\text{model}}X) \times \text{BR}(Z'_{\text{model}} \rightarrow W^+W^-)$ and $\sigma(pp \rightarrow Z'_{\text{model}}X) \times \text{BR}(Z'_{\text{model}} \rightarrow ZH)$, respectively.

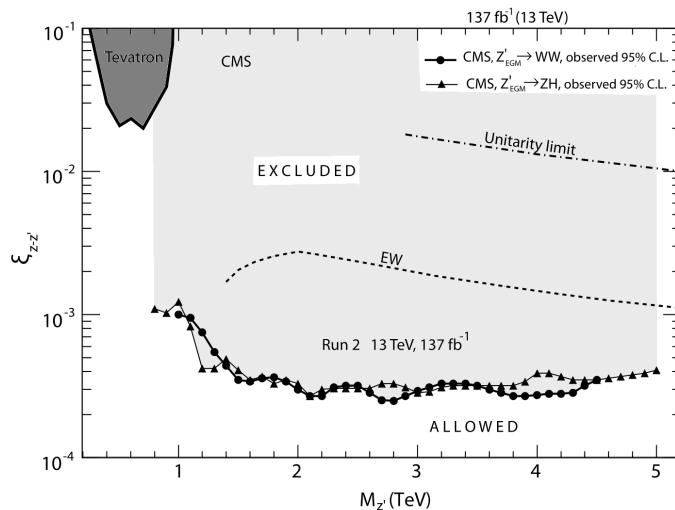


FIG. 6. The Z'_{EGM} model: 95% C.L. exclusion regions in the two-dimensional $(M_{Z'}, \xi_{Z-Z'})$ plane obtained after incorporating indirect constraints from electroweak precision data (dashed curve labeled “EW” [6]), and direct search constraints from the Tevatron in $p\bar{p} \rightarrow WZX$ (dark shaded area) [17] as well as from the LHC searches for $pp \rightarrow Z' \rightarrow WW$ and $pp \rightarrow Z' \rightarrow ZH$ in semileptonic final states using the full Run 2 CMS data set. The region above the curves for the WW and ZH channels are excluded.

V. CONCLUDING REMARKS

Exploration of the diboson WZ/WH and WW/ZH production at the LHC with the 13 TeV data set allows to place stringent constraints on the W - W' and Z - Z' mixing parameters in the resonance mass range between ~ 1.0 TeV and 4.5 TeV³. We derived such limits by using the full CMS Run 2 data set recorded at the CERN LHC, with integrated luminosity of 137 fb^{-1} . By comparing the experimental limits to the theoretical predictions for the total cross section of the W' and Z' resonant production and its subsequent decay into WZ/WH and WW/ZH pairs, $\sigma(pp \rightarrow W'X) \times \text{BR}(W' \rightarrow WZ/WH)$ vs $\sigma_{95\%} \times \text{BR}(W' \rightarrow WZ/WH)$ and $\sigma(pp \rightarrow Z'X) \times \text{BR}(Z' \rightarrow W^+W^-/ZH)$ vs $\sigma_{95\%} \times \text{BR}(Z' \rightarrow W^+W^-)$, we show that the derived limits on the mixing parameters, $\xi_{W-W'}$ and $\xi_{Z-Z'}$, for the benchmark models, are substantially improved (of the order of a few $\times 10^{-4}$) with respect to those obtained from the global analysis of low-energy electroweak data (EW), as well as from the diboson production study performed at the Tevatron and those based on the CMS Run 1 and on the CMS Run 2 at time-integrated luminosity of $\sim 36 \text{ fb}^{-1}$. Further constraining of this mixing can be achieved from the analysis of future CMS data to be collected in Run 3 as well as at the next options of hadron colliders such as HL-LHC and HE-LHC as demonstrated in [24] for the ATLAS experiment.

ACKNOWLEDGEMENTS

We would like to thank V.A. Bednyakov for helpful discussions. This research has been partially supported by the Abdus Salam ICTP (TRIL Program) and by the Belarusian Republican Foundation for Fundamental Research, F21ICR-001. The work of P.O. has been supported by the Research Council of Norway.

-
- [1] G. Altarelli, B. Mele, and M. Ruiz-Altaba, Searching for New Heavy Vector Bosons in $p\bar{p}$ Colliders, *Z. Phys. C* **45**, 109 (1989), [Erratum: *Z.Phys.C* 47, 676 (1990)].
 [2] E. Eichten, I. Hinchliffe, K. D. Lane, and C. Quigg, Super Collider Physics, *Rev. Mod. Phys.* **56**, 579 (1984), [Addendum: *Rev.Mod.Phys.* 58, 1065–1073 (1986)].

³ A slightly wider resonance mass range was taken for the process of $Z' \rightarrow ZH$, namely $0.8 - 5$ TeV.

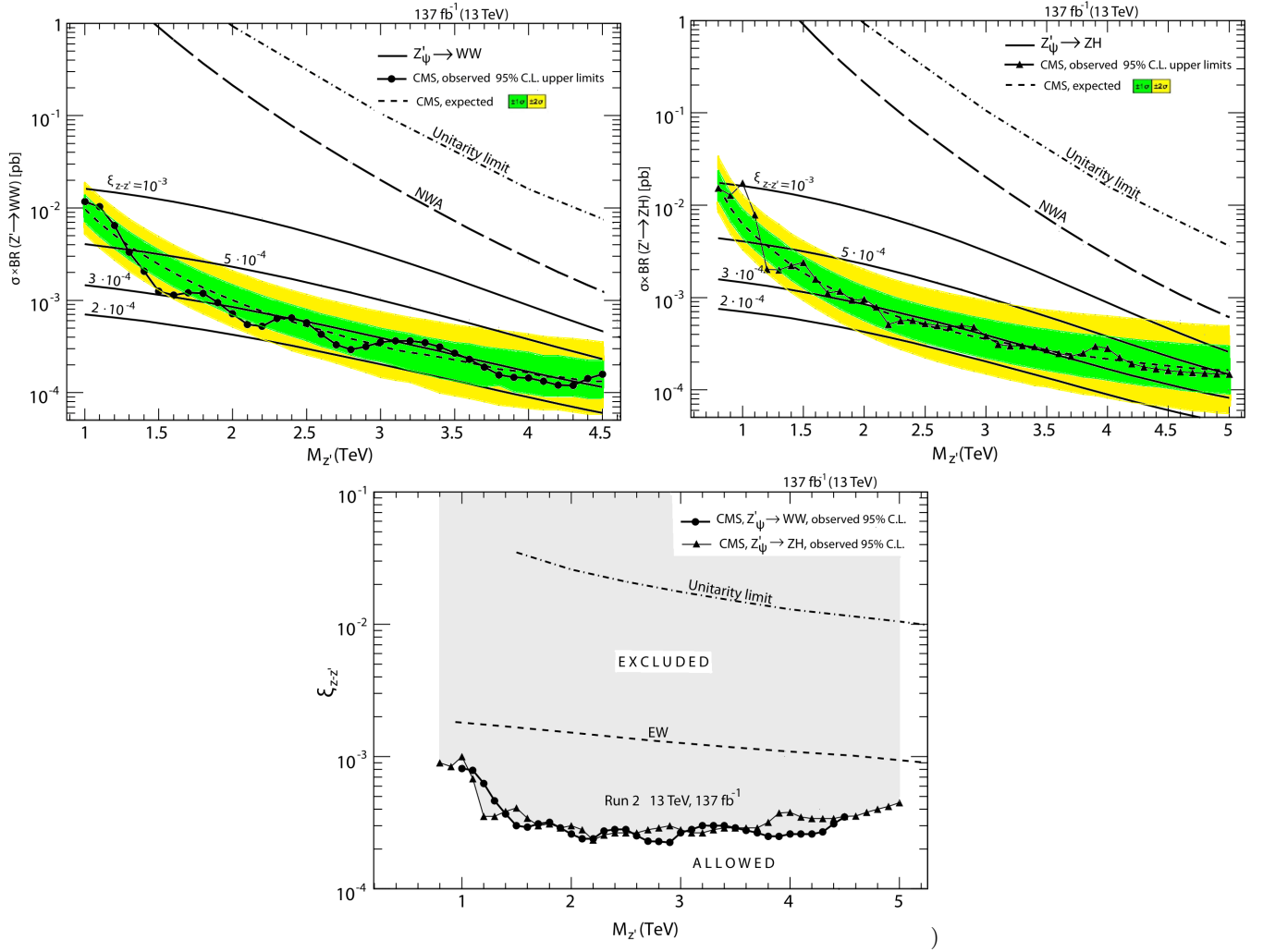


FIG. 7. $E_6 Z'_\psi$ model: Analogous to Figs. 5 and 6, respectively.

- [3] J. L. Hewett and T. G. Rizzo, Low-Energy Phenomenology of Superstring Inspired $E(6)$ Models, Phys. Rept. **183**, 193 (1989).
- [4] A. Leike, The Phenomenology of extra neutral gauge bosons, Phys. Rept. **317**, 143 (1999), arXiv:hep-ph/9805494.
- [5] P. Langacker, The Physics of Heavy Z' Gauge Bosons, Rev. Mod. Phys. **81**, 1199 (2009), arXiv:0801.1345 [hep-ph].
- [6] J. Erler, P. Langacker, S. Munir, and E. Rojas, Improved Constraints on Z' -prime Bosons from Electroweak Precision Data, JHEP **08**, 017, arXiv:0906.2435 [hep-ph].
- [7] L. Randall and R. Sundrum, A Large mass hierarchy from a small extra dimension, Phys. Rev. Lett. **83**, 3370 (1999), arXiv:hep-ph/9905221.
- [8] H. Davoudiasl, J. Hewett, and T. Rizzo, Experimental probes of localized gravity: On and off the wall, Phys. Rev. D **63**, 075004 (2001), arXiv:hep-ph/0006041.
- [9] K. Lane and S. Mrenna, The Collider Phenomenology of Technihadrons in the Technicolor Straw Man Model, Phys. Rev. D **67**, 115011 (2003), arXiv:hep-ph/0210299.
- [10] E. Eichten and K. Lane, Low-scale technicolor at the Tevatron and LHC, Phys. Lett. B **669**, 235 (2008), arXiv:0706.2339 [hep-ph].
- [11] K. Agashe, R. Contino, and A. Pomarol, The Minimal composite Higgs model, Nucl. Phys. B **719**, 165 (2005), arXiv:hep-ph/0412089.
- [12] G. F. Giudice, C. Grojean, A. Pomarol, and R. Rattazzi, The Strongly-Interacting Light Higgs, JHEP **06**, 045, arXiv:hep-ph/0703164.
- [13] D. Pappadopulo, A. Thamm, R. Torre, and A. Wulzer, Heavy Vector Triplets: Bridging Theory and Data, JHEP **09**, 060, arXiv:1402.4431 [hep-ph].
- [14] P. A. Zyla *et al.* (Particle Data Group), Review of Particle Physics, PTEP **2020**, 083C01 (2020).

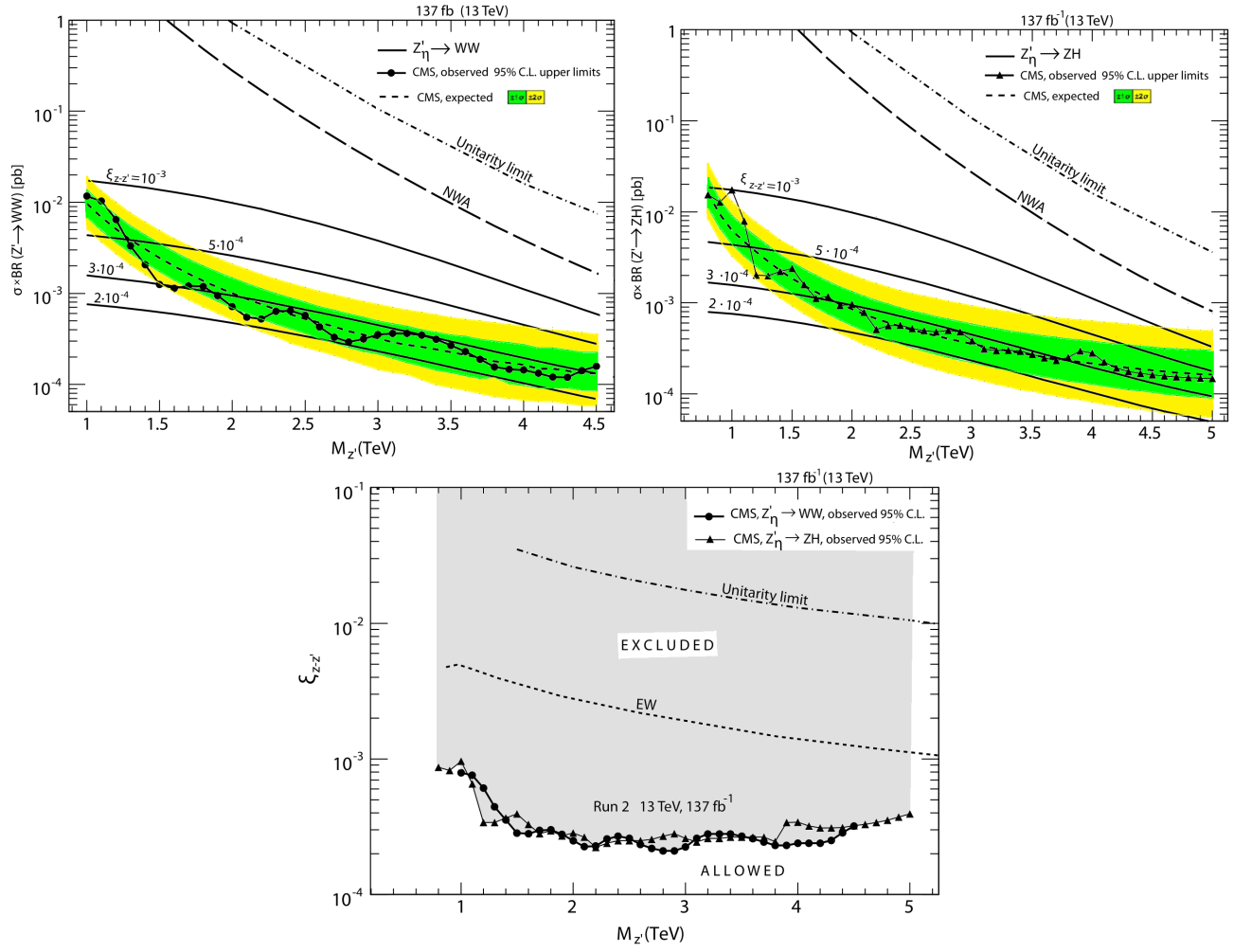


FIG. 8. $E_6 Z'_\eta$ model: Analogous to Figs. 5 and 6, respectively.

- [15] E. Salvioni, G. Villadoro, and F. Zwirner, Minimal Z-prime models: Present bounds and early LHC reach, JHEP **11**, 068, arXiv:0909.1320 [hep-ph].
- [16] A. Gulov, A. Pankov, A. Pevzner, and V. Skalozub, Model-independent constraints on the Abelian Z' couplings within the ATLAS data on the dilepton production processes at $\sqrt{s} = 13$ TeV, Nonlin. Phenom. Complex Syst. **21**, 21 (2018), arXiv:1803.07532 [hep-ph].
- [17] T. Aaltonen et al. (CDF), Search for WW and WZ Resonances Decaying to Electron, Missing E_T , and Two Jets in $p\bar{p}$ Collisions at $\sqrt{s} = 1.96$ TeV, Phys. Rev. Lett. **104**, 241801 (2010), arXiv:1004.4946 [hep-ex].
- [18] P. Osland, A. Pankov, and A. Tsytrinov, Probing Z - Z' mixing with ATLAS and CMS resonant diboson production data at the LHC at $\sqrt{s} = 13$ TeV, Phys. Rev. D **96**, 055040 (2017), arXiv:1707.02717 [hep-ph].
- [19] I. Bobovnikov, P. Osland, and A. Pankov, Improved constraints on the mixing and mass of Z' bosons from resonant diboson searches at the LHC at $\sqrt{s} = 13$ TeV and predictions for Run II, Phys. Rev. D **98**, 095029 (2018), arXiv:1809.08933 [hep-ph].
- [20] I. Serenkova, P. Osland, and A. Pankov, Improved bounds on W - W' mixing with ATLAS resonant WZ production data at the LHC at $\sqrt{s} = 13$ TeV, Phys. Rev. D **100**, 015007 (2019), arXiv:1904.01432 [hep-ph].
- [21] M. Aaboud et al. (ATLAS), Search for WW/WZ resonance production in $\ell\nu qq$ final states in pp collisions at $\sqrt{s} = 13$ TeV with the ATLAS detector, JHEP **03**, 042, arXiv:1710.07235 [hep-ex].
- [22] A. M. Sirunyan et al. (CMS), Search for massive resonances decaying into WW , WZ , ZZ , qW , and qZ with dijet final states at $\sqrt{s} = 13$ TeV, Phys. Rev. D **97**, 072006 (2018), arXiv:1708.05379 [hep-ex].
- [23] A. Pankov, P. Osland, I. Serenkova, and V. Bednyakov, High-precision limits on W - W' and Z - Z' mixing from diboson production using the full LHC Run 2 ATLAS data set, Eur. Phys. J. C **80**, 503 (2020), arXiv:1912.02106 [hep-ph].
- [24] P. Osland, A. A. Pankov, and I. A. Serenkova, Updated constraints on Z' and W' bosons decaying into bosonic and leptonic final states using the run 2 ATLAS data, Phys. Rev. D **103**, 053009 (2021), arXiv:2012.13930 [hep-ph].

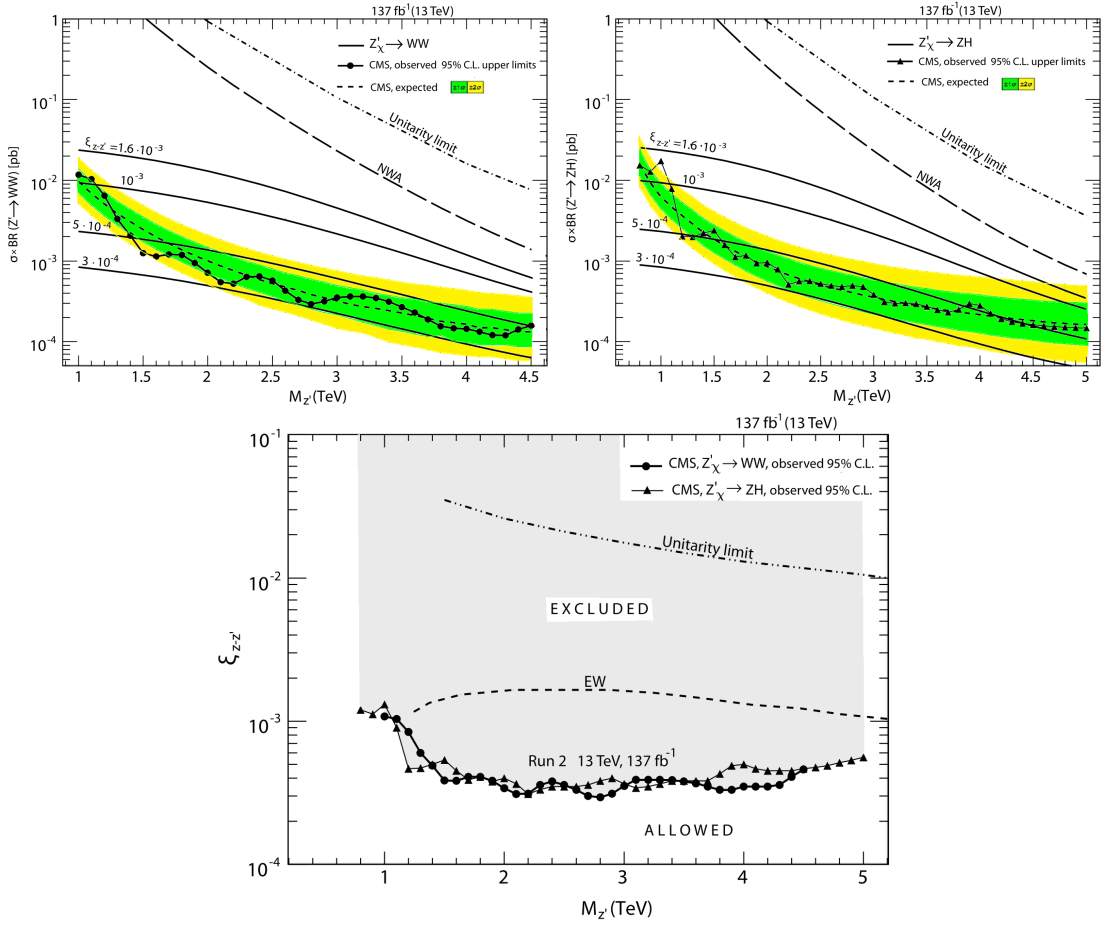


FIG. 9. $E_6 Z'_X$ model: Analogous to Fig. 5 and Fig. 6, respectively.

- [25] G. Aad et al. (ATLAS), Search for heavy diboson resonances in semileptonic final states in pp collisions at $\sqrt{s} = 13$ TeV with the ATLAS detector, *Eur. Phys. J. C* **80**, 1165 (2020), arXiv:2004.14636 [hep-ex].
- [26] A. Tumasyan et al. (CMS), Search for heavy resonances decaying to WW , WZ , or WH boson pairs in the lepton plus merged jet final state in proton-proton collisions at $\sqrt{s} = 13$ TeV, *Phys. Rev. D* **105**, 032008 (2022), arXiv:2109.06055 [hep-ex].
- [27] Durham Hepdata repository, <https://www.hepdata.net/record/ins102645> (2021).
- [28] A. M. Sirunyan et al. (CMS), Search for a heavy vector resonance decaying to a Z boson and a Higgs boson in proton-proton collisions at $\sqrt{s} = 13$ TeV, *Eur. Phys. J. C* **81**, 688 (2021), arXiv:2102.08198 [hep-ex].
- [29] Durham Hepdata repository, <https://www.hepdata.net/record/ins101374> (2021).
- [30] P. Langacker and M.-x. Luo, Constraints on additional Z bosons, *Phys. Rev. D* **45**, 278 (1992).
- [31] A. Djouadi, A. Leike, T. Riemann, D. Schaile, and C. Verzegnassi, Signals of new gauge bosons at future e^+e^- colliders, *Z. Phys. C* **56**, 289 (1992).
- [32] C. Grojean, E. Salvioni, and R. Torre, A weakly constrained W' at the early LHC, *JHEP* **07**, 002, arXiv:1103.2761 [hep-ph].
- [33] B. A. Dobrescu and Z. Liu, Heavy Higgs bosons and the 2 TeV W' boson, *JHEP* **10**, 118, arXiv:1507.01923 [hep-ph].
- [34] M. S. Chanowitz and M. K. Gaillard, The TeV Physics of Strongly Interacting W 's and Z 's, *Nucl. Phys. B* **261**, 379 (1985).
- [35] A. Alves, O. Eboli, D. Goncalves, M. Gonzalez-Garcia, and J. Mizukoshi, Signals for New Spin-1 Resonances in Electroweak Gauge Boson Pair Production at the LHC, *Phys. Rev. D* **80**, 073011 (2009), arXiv:0907.2915 [hep-ph].
- [36] T. Sjöstrand, S. Ask, J. R. Christiansen, R. Corke, N. Desai, P. Ilten, S. Mrenna, S. Prestel, C. O. Rasmussen, and P. Z. Skands, An introduction to PYTHIA 8.2, *Comput. Phys. Commun.* **191**, 159 (2015), arXiv:1410.3012 [hep-ph].
- [37] R. Hamberg, W. van Neerven, and T. Matsuura, A complete calculation of the order α_s^2 correction to the Drell-Yan K factor, *Nucl. Phys. B* **359**, 343 (1991), [Erratum: *Nucl. Phys. B* **644**, 403–404 (2002)].
- [38] S. Chatrchyan et al. (CMS), Search for a W' or Techni- ρ Decaying into WZ in pp Collisions at $\sqrt{s} = 7$ TeV, *Phys. Rev. Lett.* **109**, 141801 (2012), arXiv:1206.0433 [hep-ex].
- [39] V. Khachatryan et al. (CMS), Search for New Resonances Decaying via WZ to Leptons in Proton-Proton Collisions at $\sqrt{s} = 8$ TeV, *Phys. Lett. B* **740**, 83 (2015), arXiv:1407.3476 [hep-ex].

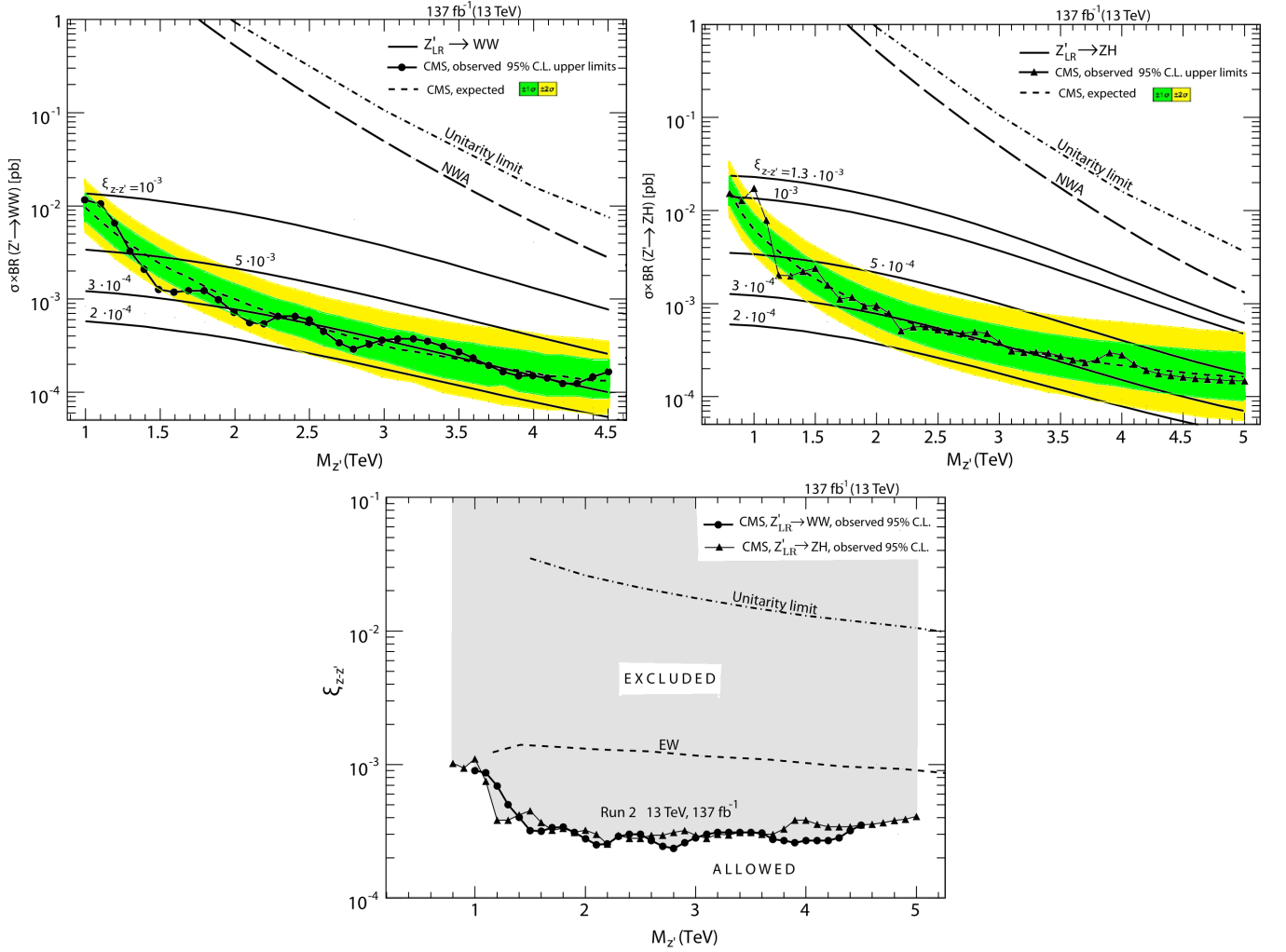


FIG. 10. Z'_{LR} model: Analogous to Fig. 5 and Fig. 6, respectively.

- [40] G. Aad et al. (ATLAS), Search for resonant diboson production in the $WW/WZ \rightarrow \ell\nu jj$ decay channels with the ATLAS detector at $\sqrt{s} = 7$ TeV, Phys. Rev. D **87**, 112006 (2013), arXiv:1305.0125 [hep-ex].
- [41] V. D. Barger and K. Whisnant, Heavy Z Boson Decays to Two Bosons in $E(6)$ Superstring Models, Phys. Rev. D **36**, 3429 (1987).
- [42] V. Barger, P. Langacker, and H.-S. Lee, Six-lepton Z -prime resonance at the LHC, Phys. Rev. Lett. **103**, 251802 (2009), arXiv:0909.2641 [hep-ph].
- [43] C. Dib and F. J. Gilman, Extra Neutral Gauge Bosons in Electron - Positron Collisions at Resonance, Phys. Rev. D **36**, 1337 (1987).
- [44] A. M. Sirunyan et al. (CMS), Combination of searches for heavy resonances decaying to WW , WZ , ZZ , WH , and ZH boson pairs in proton-proton collisions at $\sqrt{s} = 8$ and 13 TeV, Phys. Lett. B **774**, 533 (2017), arXiv:1705.09171 [hep-ex].
- [45] S. Frixione, A Next-to-leading order calculation of the cross-section for the production of $W^+ W^-$ pairs in hadronic collisions, Nucl. Phys. B **410**, 280 (1993).
- [46] N. Agarwal, V. Ravindran, V. K. Tiwari, and A. Tripathi, Next-to-leading order QCD corrections to $W^+ W^-$ production at the LHC in Randall Sundrum model, Phys. Lett. B **690**, 390 (2010), arXiv:1003.5445 [hep-ph].
- [47] T. Gehrmann, M. Grazzini, S. Kallweit, P. Maierhöfer, A. von Manteuffel, S. Pozzorini, D. Rathlev, and L. Tancredi, $W^+ W^-$ Production at Hadron Colliders in Next to Next to Leading Order QCD, Phys. Rev. Lett. **113**, 212001 (2014), arXiv:1408.5243 [hep-ph].